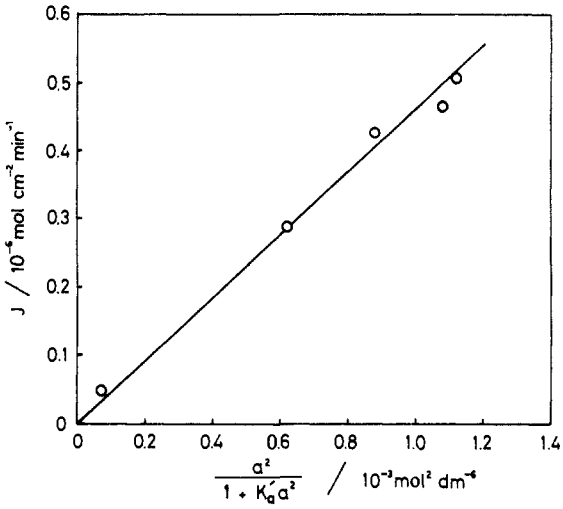

Figure 7. J vs. $a^2/(1 + K_a'a^2)$ plot for the polynactin-KSCN system. [PN] = 0.1 mol dm^{-3}.

discrepancy may be due to a difference in the stirring conditions between the ion-transfer and ion-transport experiments. If the two experiments could be carried out under the same stirring conditions, a theoretical curve for ion transport might be drawn by use of the apparent rate constant derived from ion-transfer experiments.

For all the carriers studied here, the value of k_r is comparable to that of k_u, so that the rate of release does not control the overall rate of transport. When log K_e is higher than 4-6 for a monovalent cation, the rate of transport decreases with an increase in K_e as demonstrated by Behr and co-workers.[7] The rate of release decreases with an increase in the stability constant of the complex and controls the rate of transport in the region of high stability.[16] When K_e is very high, the concentration of the complex at the interface on the release side ($\bar{c}_M$*) is not longer negligible in comparison with the concentration in the bulk solution ($\bar{c}_M$). Under these circumstances, we have to use eq 12, or $J_r = k_r'\bar{c}_M$ where $k_r' = k_r(1 - \bar{c}_M^*/\bar{c}_M)$; the k_r' apparently decreases with an increase in $\bar{c}_M$*. The k_r' values, calculated from J_r values previously determined for potassium picrate,[16,17] were 0.27×10^{-4} and 0.82×10^{-4} cm s^{-1} for cryptand 2.2.2 and dibenzocryptand 2.2.2, respectively. These values are 1-2 orders of magnitude lower than those for crown ethers. In such a case, the transport of the ion does not proceed so fast as would be expected from its high affinity to the carrier. However, most of the metal complexes with macrocyclic ligands exhibit log K_e of 4-6 or lower,[10-13] so that the rate of transport is predictable from the extractability of the metal ion.

Acknowledgment. We are grateful to Chugai Pharmaceutical Co., Ltd., for kindly supplying us with polynactin, and to H. Inoue, T. Takahashi, and S. Tanaka for their assistance in the experiments.

(16) Yoshida, S.; Hayano, S. *J. Membr. Sci.* **1986**, *26*, 99-106.
(17) When $\bar{c}_M$ was 1×10^{-3} mol dm^{-3}, the J_r values were 1.6×10^{-9} and 4.9×10^{-9} mol min^{-1} cm^{-2} for cryptand 2.2.2 and dibenzocryptand 2.2.2, respectively.
(18) Shchori, E.; Nae, N.; Grodzinski, J. J. *J. Chem. Soc., Dalton Trans.* **1975**, 2381-2386.
(19) Izatt, R. M.; Nelson, D. P.; Rytting, J. H.; Haymore, B. L.; Christensen, J. J. *J. Am. Chem. Soc.* **1971**, *93*, 1619-1623.
(20) Frensdorff, H. K. *J. Am. Chem. Soc.* **1971**, *93*, 600-606.

Analysis of the Absorption and Fluorescence Spectra of Trimethylamine: Determination of the $\tilde{A}$-$\tilde{X}$ Origin and the Ground-State Inversion Barrier

Arthur M. Halpern,* Mary Jo Ondrechen, and Lawrence D. Ziegler

Contribution from the Department of Chemistry, Northeastern University, Boston, Massachusetts 02115. *Received December 26, 1985*

Abstract: The second derivative of the gas-phase absorption spectrum of trimethylamine (TMA) is used to assign the positions of many vibrational features in the $\tilde{A} \leftarrow \tilde{X}$ transition. Considerable regularity in these positions indicates that the $\tilde{A}$ state potential is harmonic in the out-of-plane bending coordinate, and a frequency of 375 cm^{-1} is assigned. Calculations based on the finite difference method using an $\tilde{X}$-state inversion potential of local harmonic wells joined by a parabolic or quartic cap and a harmonic $\tilde{A}$ state are successfully used to fit the shapes of both the absorption and fluorescence spectra. Most of the Franck-Condon activity in fluorescence involves transitions to the $v'' = 14$-18 states, explaining the large Stokes' shift as well as the vertical shape. The origin of the $\tilde{A} \leftarrow \tilde{X}$ transition is assigned at 37 550 cm^{-1}, and the inverion barrier height is estimated to be 2900 cm^{-1} based on a parabolic- or quartic-capped pair of harmonic wells. Comparisons are made with calculated TMA inversion barriers.

Electronic transitions between potential energy surfaces that are severely distorted and displaced from each other serve as a sensitive probe of the characteristics of these surfaces. Thus absorption and emission band shapes can reveal detailed information about potential energy surfaces possessing multiple minima which are ubiquitous in applications to chemical structure and reactivity. One classic example concerns the ground and excited electronic states of ammonia, the former of which is characterized by the well-known double minimum inversion potential. The pyramidal to planar structural change that accompanies electronic excitation in ammonia lends a degree of richness and complexity to its spectroscopy that has been the focus of intense interest from the microwave to the UV region for many years.[1] The same fundamental structural properties that attend to the upper and lower electronic states in ammonia apply as well to trimethylamine

(1) (a) Douglas, A. E. *Discuss. Faraday Soc.* **1963**, *35*, 158. (b) Walsh, A. D.; Warsop, P. A. *Trans. Faraday Soc.* **1961**, *57*, 345. (c) Ziegler, L. D.; Hudson, B. *J. Phys. Chem.* **1984**, *88*, 1110. (d) Vaida, V.; Hess, W.; Roebber, J. L. *J. Phys. Chem.* **1984**, *88*, 3397.

0002-7863/86/1508-3907$01.50/0

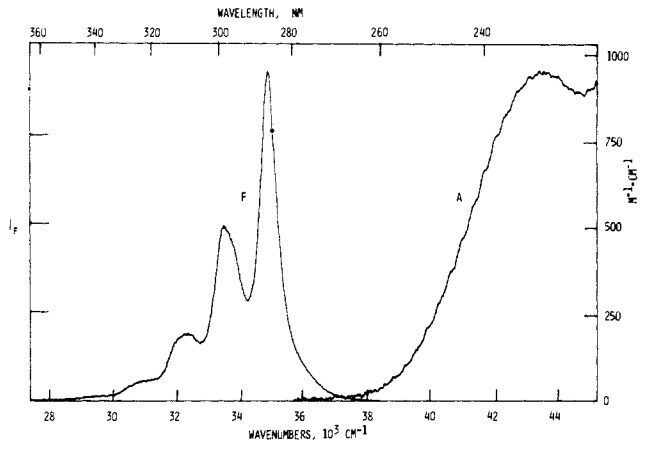

Figure 1. Vapor-phase absorption (A) and fluorescence (F) spectra of TMA. For (F), 100 torr of 2-methylbutane was used to ensure vibrational relaxation.

(TMA), the simplest tertiary organic amine.[2] This compound, unlike ammonia and primary and secondary amines, which undergo efficient excited state N–H photodissociation, relaxes radiatively from its lowest lying electronic state.[3,4] Therefore both absorption and fluorescence can be used to probe the excited and ground potential energy surfaces in TMA.

The ultraviolet absorption spectrum of TMA vapor reveals two maxima, at 227 and 198 nm. These transitions have been assigned as Rydberg in nature, the lower lying one as $3s \leftarrow n_N$ ($\tilde{A}\,^1A_2'' \leftarrow \tilde{X}\,^1A_1$), and the other, more intense transition as $3p_{xy,z} \leftarrow n_N$ ($\tilde{B}$, $\tilde{C}\,^1E''$, $^1A_1' \leftarrow \tilde{X}\,^1A_1$).[5] The shapes of these absorption bands are consistent with transitions between severely displaced potential energy surfaces. The electronic origin of the $\tilde{A} \leftarrow \tilde{X}$ transition is, at best, indistinct, and the absorption maximum lies several thousand wavenumbers to the blue of the onset of absorption. The envelope of this spectrum, which is nearly totally devoid of vibrational structure, is typical of a Franck–Condon (FC)-restricted transition. The value of the oscillator strength (0.0177)[6] indicates that the transition is formally allowed.

The fluorescence spectrum of TMA, on the other hand, appears distinctly different from the $\tilde{A} \leftarrow \tilde{X}$ transition. Shown in Figure 1, it exhibits a relatively narrow feature at 287 nm that, when considered with the other vibronic features at lower energy, actually resembles a 0–0 band. In other words, the fluorescence appears vertical in nature in contradistinction to the absorption spectrum. While the FC envelopes of these spectra are disparate, there is no evidence that the fluorescence originates from an excited electronic state other than than A_2''. The value of the radiative rate constant (2.1×10^7 s^{-1})[3] is consistent with the integrated absorption strength estimated for the $\tilde{A} \leftarrow \tilde{X}$ transition.[6,7] Moreover, there is consistency between the fluorescence excitation and the $\tilde{A} \leftarrow \tilde{X}$ absorption spectra.[8] Furthermore, the multiphoton ionization spectrum of TMA does not reveal the presence of any other dipole-forbidden electronic transition in the vicinity of the $\tilde{A} \leftrightarrow \tilde{X}$ transitions.[9] While these observations are not necessarily definitive, the weight of evidence nevertheless allows one to rule out a "hidden transition" such as found in the linear polyenes[10] as being the cause of the discrepancy between the absorption and fluorescence spectra of TMA.

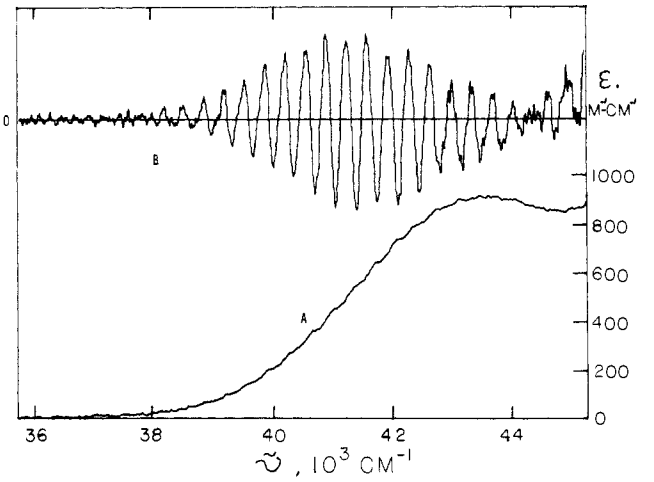

Figure 2. Absorption spectrum of TMA (A) and its second derivative (B) obtained at 4 torr, 1-cm pathlength.

Table I. Positions of the SD Maxima in the TMA Absorption Spectrum

nm[a]	cm^{-1}[b]	nm	cm^{-1}	nm	cm^{-1}
276.8	36 127	249.2	40 128	223.8	44 683
274.2	36 470	246.7	40 531	222.1	45 025
271.7	36 805	244.6	40 883	220.5	45 351
269.0	37 175	242.3	41 271	218.7	45 725
(267.6)	37 369	240.2	41 632	217.1	46 062
266.4	37 537	238.0	42 017	215.5	46 404
263.8	37 908	235.9	42 391	214.0	46 729
261.4	38 256	233.9	42 753	212.6	47 037
(259.0)	38 610	231.7	43 159	211.2	47 349
258.6	38 670	229.7	43 535	209.7	47 687
256.4	39 002	227.6	43 937	208.4	47 985
254.0	39 370	225.6	44 326	207.7	48 146
(251.5)	39 761				

[a] ±0.1 nm. [b] ±20 cm^{-1}.

The peculiar appearance of the $\tilde{A} \leftrightarrow \tilde{X}$ spectra has been noted before, and it has been suggested that the vertical pattern of the fluorescence spectrum (at least the first prominant feature at 287 nm) arises from transitions from the thermally equilibrated excited state to ground-state vibrational levels near the top of the potential barrier separating the two equivalent pyramidal forms of TMA.[11] This paper reports the results of calculations that confirm this hypothesis. Our calculations are based upon simple model potentials obtained from a very careful reexamination of the experimental spectra. In addition, the results show that a rather precise assignment of the barrier to inversion in TMA can be made. The origin of the $\tilde{A} \leftarrow \tilde{X}$ transition is also assigned on the basis of these calculations and in concert with experimental results.

Results and Discussion

Absorption Spectrum. As can be seen in Figure 1, the $\tilde{A} \leftarrow \tilde{X}$ absorption spectrum of TMA is vibrationally diffuse. As reported by Matsumi and Obi, however, some evidence of vibronic structure can be discerned from the subtle undulations in the spectrum, especially on the low-energy end.[8] These features can be remarkably enhanced by obtaining the derivative spectra of TMA. The second derivative (SD) spectrum of TMA vapor at a pressure of 4.0 torr (path length 1.00 cm) is shown superimposed with the ordinary absorption spectrum in Figure 2. Model

(2) Kasatani, K.; Kawasaki, M.; Sato, H.; Murasawa, Y.; Obi, K.; Tanaka, I. *J. Chem. Phys.* **1981**, *74*, 3164.
(3) Halpern, A. M.; Gartman, T. *J. Am. Chem. Soc.* **1974**, *96*, 1393.
(4) Freeman, C. G.; McEwan, M. J.; Clairidge, R. F. C.; Phillips, L. F. *Chem. Phys. Lett.* **1971**, *8*, 77.
(5) (a) Kawasaki, M.; Kasatani, K.; Sato, H.; Shinohara, H.; Nishi, N.; Ibuki, T. *J. Chem. Phys.* **1982**, *77*, 258. (b) Robin, M. B. *Higher Excited States of Polyatomic Molecules*; Academic: New York, 1974; Vol. 1, pp 208–229.
(6) The oscillator strength was determined from the low-pressure fluorescence excitation spectrum, which was normalized to quantitative absorption at 240 nm. This approach presumably captures the true $\tilde{A} \leftarrow \tilde{X}$ absorption strength.
(7) On the basis of the integrated absorption, the calculated value of the TMA radiative rate constant was determined to be 2.2×10^7 s^{-1}.
(8) Matsumi, Y.; Obi, K. *Chem. Phys.* **1980**, *49*, 87.
(9) (a) Halpern, A. M.; Gerrity, D. J.; Rothman, L. J.; Vaida, V. *J. Chem. Phys.* **1982**, *76*, 102. (b) Parker, D. H.; Bernstein, R. B.; Lichtin, D. A. *Ibid.* **1981**, *75*, 2577.
(10) Hudson, B. S.; Kohler, B. E.; Schulton, K. In *Excited States*; Lim, E. C., Ed.; Academic: New York, 1982; Vol. 6, pp 1–95.
(11) Halpern, A. M. In *The Chemistry of the Functional Groups*; Patai, S., Ed.; Wiley: Chichester, 1982; Supplement F, Part 2, Chapter 5, pp 155–180.

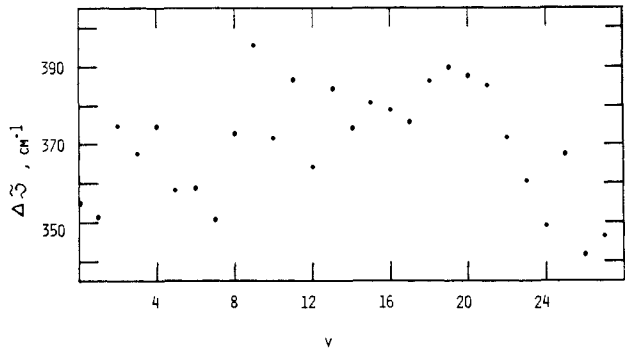

Figure 3. Plot of $\Delta\tilde{\nu}$ *vs* v for the second-derivative features. Estimated uncertainty in $\Delta\tilde{\nu}$ is ± 20 cm^{-1}.

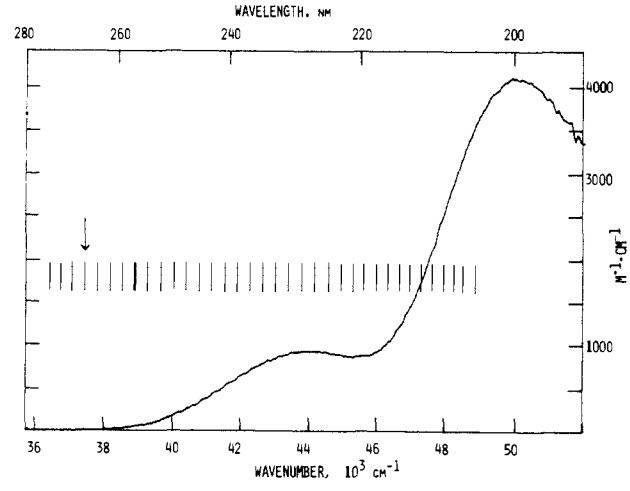

Figure 4. Absorption of TMA vapor at 300 K. The lines represent the positions of the second derivative maxima.

calculations show that the SD spectrum of Gaussian-broadened sticks, designed to represent the observed spectrum of TMA, produces maxima (or minima) at, or very near, the stick positions. Hence, the positions of (in this case) the maxima in the SD spectrum can be used to assign the positions of the vibrational structure in the TMA absorption spectrum. Furthermore, by varying the pressure and path length of the TMA sample, and hence the wavelength region in which the optical density manifests an appropriate change, SD features can be recorded over a very wide range of the TMA absorption spectrum. Features as far to the red as 287.3 nm (i.e., at the strongest fluorescence feature) can be clearly revealed via the SD approach (vide infra). Table I summarizes the wavelength and wavenumber positions of the SD features assigned in the TMA spectrum, and a plot of $\Delta\tilde{\nu}$ vs. v is shown in Figure 3. Lines representing these features are superimposed on the absorption spectrum in Figure 4. It will be shown below that one of these features can be assigned as the origin of the $\tilde{A} \leftarrow \tilde{X}$ transition.

The regularity in the positions of the SD-based vibrational assignments, as well as the smooth intensity pattern, strongly suggests that the potential energy surface of the $\tilde{A}$ state of TMA (along the relevant degree of freedom) can be represented as a harmonic potential. The mean value of the vibrational spacings thus analyzed is 375 cm^{-1} $\pm$ 10 cm^{-1} (see Figure 4) and compares well with that estimated by Matsumi and Obi (380 cm^{-1}).[8] It seems reasonable to assume that the degree of freedom represented by this vibrational progression is the out-of-plane bending of TMA. In the ground state, this mode (ν_7) is assigned a frequency of 365 cm^{-1}.[12] The prominence of this mode in the TMA absorption spectrum is also consistent with the analogous $\tilde{A} \leftarrow \tilde{X}$ transition in ammonia.[1]

(12) (a) Gayles, J. N. *Spectrochim. Acta* **1967**, *23A*, 1531. (b) Dellepiani, G.; Zerbi, G. *J. Chem. Phys.* **1968**, *48*, 3753.

The similarity in ν_7 values for the $\tilde{A}$ and $\tilde{X}$ states in TMA is noteworthy in view of the large difference in shape of the bending potentials of the electronic surfaces, as well as the significant displacement in the minima of these potentials. This effect is analogously observed in NH_3, for which $\tilde{A}$ and $\tilde{X}$ state bending frequencies are 900[1d] and 950 cm^{-1}, respectively. It would thus appear that for these amines the bending potential is very insensitive to the hybridization of the nonbonding electrons; hence, electronic excitation has little effect on the restoring force for this motion. This suggests that the bending potential surface is primarily influenced by the σ-bonding electrons in the N–(CH_3) (or H) moieties.

In attempting to account for the shape of the $\tilde{A} \leftarrow \tilde{X}$ absorption spectrum in TMA, we will adopt a one-dimensional potential in which the degree of freedom is the out-of-plane bending coordinate. While an analysis of the TMA fluorescence clearly indicates the activity of other modes (involving stretching and bending), we nevertheless use a ν_7-based potential to see whether the general vertical-like appearance of the 287-nm feature can be accounted for with this simple model.

We assume in the treatment that follows that the electronic transition moment for $\tilde{A} \leftarrow \tilde{X}$ is independent of nuclear coordinates and thus that the transition probability between lower and upper vibrational states v' and v'', respectively, is proportional to the FC factor, $\langle v'|v''\rangle^2$. The absorption (or fluorescence) intensity of the transition between v′ and v″ is then proportional to the FC factor multiplied by the Boltzmann factor, $\exp\{-E(v)/kT\}$, where $E(v)$ is the eigenvalue of the v''th (or v'th) state.

FC factors were determined by the numerical integration of the appropriate wavefunctions, which were obtained by solving the Schrödinger equation with a finite-difference method. The advantage of this straightforward approach is that eigenvectors and eigenvalues can be obtained for any arbitrary one-dimensional potential energy function as long as it spans a sufficiently large range of the space coordinate. A brief description of this method is outlined in the Appendix. In these calculations, potential energy functions spanning a range of 180 points in the inversion or out-of-plane bending coordinate were used; accordingly, eigenfunctions having a density of 180 points in this coordinate were obtained. It was determined that the upper and lower state eigenvalues, as well as the relevant FC factors, were convergent for this number of points.

In carrying out these calculations, the following simplifying assumptions were made: (1) the methyl groups were treated as point masses, and (2) the C–N bond lengths, L, were assumed to be equal and constant (1.472 Å).[13] As a consequence of (1), methyl rotations were not treated explicitly but were dealt with empirically (vide infra). From (2), the reduced mass of TMA is independent of the bending coordinate and was determined as $3\text{Me}/[1 + (3\text{Me}/N)]$, where Me and N are the masses of the methyl group and nitrogen atom, respectively.

In choosing a one-dimensional potential to account for the large-amplitude vibration in the inversion mode, we examined the various anharmonic double-minima potentials that have previously been applied to ammonia.[14] However, to treat the ground state of TMA we decided to use a potential based on two local parabolic wells smoothly joined by a quadratic (or quartic) cap.[15] The rationale for this choice stems from the fact that there are approximately seven vibrational levels below the barrier and thus the lower lying inversion states are probably rather harmonic. The regular spacings observed in the SD spectrum also imply considerable harmonic character to the ground-state potential. The heavy CH_3 groups preclude appreciable tunneling for the lower lying vibrational states.

(13) Lide, D. R., Jr.; Mann, D. E. *J. Chem. Phys.* **1958**, *28*, 572.
(14) (a) Manning, M. F. *J. Chem. Phys.* **1935**, *3*, 136. (b) Kincaid, J. F.; Henriques, F. C., Jr. *J. Am. Chem. Soc.* **1940**, *62*, 1474. (c) Costain, C. C.; Sutherland, G. B. B. M. *J. Phys. Chem.* **1951**, *56*, 321. (d) Swalen, J. D.; Ibers, J. A. *J. Chem. Phys.* **1962**, *36*, 1914. (e) Harmony, M. D. *Chem. Phys. Lett.* **1971**, *15*, 337.
(15) Lister, D. G.; Macdonald, J. N.; Owen, N. L., *Internal Rotation and Inversion*; Academic: London, 1978; Chapter 7.

Table II. Calculated $\langle v''|0\rangle^2$ FC Factors for TMA

Ground-State ν_7 Bending Level, v''				
0	1	2	3	4
5	6	7	8	9
10	11	12	13	14
15	16	17	18	19
20	21	22	23	24
		$\langle v''\|0\rangle^2$		
5.78×10^{-7}	3.6×10^{-12}	9.11×10^{-6}	2.6×10^{-14}	7.41×10^{-5}
3.4×10^{-16}	4.24×10^{-4}	2.5×10^{-19}	2.00×10^{-3}	1.3×10^{-18}
8.76×10^{-3}	2.6×10^{-26}	3.88×10^{-2}	3.7×10^{-26}	0.175
2.6×10^{-28}	0.452	1.1×10^{-26}	0.253	7.9×10^{-27}
5.62×10^{-2}	6.7×10^{-27}	1.13×10^{-2}	9.5×10^{-27}	2.27×10^{-3}

We also found that the TMA pyramid height, x, could adequately represent the coordinate of this potential, which is expressed as

$$V(x) = A - Bx^n \quad \text{for } |x| < x'$$
$$= K''(x - x_0)^2 \quad \text{for } |x| > x' \qquad (1)$$

where A is the inversion barrier height, B and x' are parameters that depend on A, K'', and x_0,[16] and $n = 2$ or 4. K'' is an effective force constant and x_0 is the equilibrium ground-state pyramid height (for which a value of 0.50905 Å was used).[13] K'' was chosen to give low-lying ground-state eigenvalues that are consistent with the observed ν_7 value of 365 cm^{-1}. It should be emphasized that $V(x)$ is a two-parameter potential. The parameters K'' and A were chosen to fit the observed experimental data.

For the $\tilde{A}$ state, the harmonic potential $V(x) = K'x^2$ was employed, and K' as chosen to provide eigenvalues consistent with experiment, i.e., ca. 375 cm^{-1} (vide supra).

Calculated absorption spectra were constructed by superimposing Gaussian functions centered on the intensity sticks which had amplitudes, $I_{v'v''}$ given by

$$I_{v'v''} = B_{v'}FC_{v'v''}$$

where $B_{v'}$ and $FC_{v'v''}$ are the *Boltzmann* and Franck–Condon factors defined above. In these calculations the lowest 24 eigenvalues and eigenfunctions of the ground and excited states were used. Fluorescence spectra were determined in the analogous way, except that the Boltzmann factor referenced the excited-state eigenvalues.

The appropriate Gaussian width was estimated in constructing the absorption spectrum and the observed absorption spectrum was decomposed into Gaussian components. At 300 K this was determined to be ca. 460 cm^{-1}.

It should be pointed out in this context that an attempt was made to obtain an absorption spectrum of TMA vapor under low-temperature conditions in order to see whether the vibronic features would appear sharper, thus allowing a more definitive comparison with the calculated spectrum to be made. Both the direct absorption spectrum[17] and the fluorescence excitation spectrum of TMA in a jet-cooled molecular beam failed to reveal significant sharpening. The vibronic components of the absorption spectrum of TMA under static cell conditions at 180 K were found to be similar to those observed in the jet-cooled spectra and had line widths estimated to be ca. 400 cm^{-1}. We believe that the reason for this apparently large intrinsic line width in TMA is the result of differences in the methyl rotational barriers in the $\tilde{A}$ and $\tilde{X}$ states, and these differences will be discussed below. In a sense, the imposition of the 460-cm^{-1} line width on the stick spectrum (at 300 K) attempts to account for the coupling of the methyl rotations in the $\tilde{A} \leftarrow \tilde{X}$ transition.

As can be seen in Figure 1, the more strongly absorbing transition to the $3p_{xy,z}$ state(s) distorts the appearance of the $\tilde{A} \leftarrow \tilde{X}$ transition, expecially at shorter wavelengths. The problem therefore arises as to how to correct the $\tilde{A} \leftarrow \tilde{X}$ transition to allow meaningful comparison with the calculated absorption spectrum to be made. Matsumi and Obi[8] and Cureton et al.[18] have reported that the fluorescence quantum efficiency of TMA vapor, under collision-free conditions, falls dramatically for excitation wavelengths below ca. 230 nm, the point at which transitions to the $3p_{xy,z}$ state(s) commence. This falloff in fluorescence efficiency has been interpreted in terms of rapid nonradiative decay from levels in the $\tilde{A}$ state produced immediately subsequent to internal conversion from the photoexcited $3p_{xy,z}$ state(s).[8,18] We took advantage of this property by using the appearance of the fluorescence excitation (FE) spectrum of TMA under isolated conditions to be a representation of the true $\tilde{A} \leftarrow \tilde{X}$ transition profile.[6]

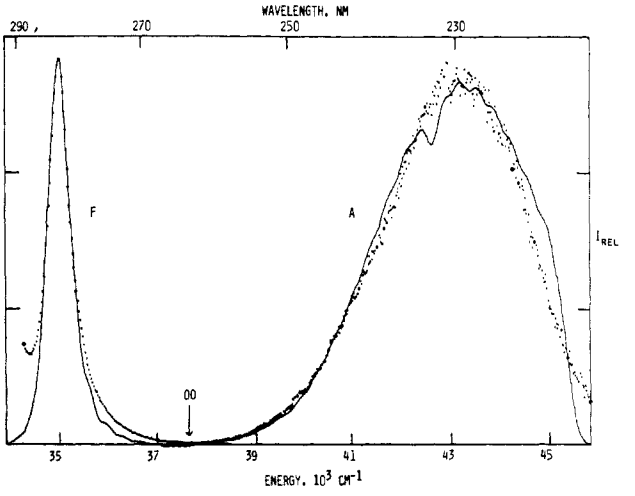

Figure 5. (A) Fluorescence excitation spectrum of TMA under isolated conditions (···), and calculated absorption spectrum (—). (F) Portion of the observed fluorescence spectrum (vibrationally relaxed) (···), and calculated fluorescence spectrum using potentials described in the text (—). Transition origin is indicated by the arrow.

The absorption spectrum produced by the Gaussian-broadened sticks based on the wavefunctions for the upper and lower states described above fits the observed FE spectrum rather well. This comparison is shown on the right-hand side of Figure 5. It is interesting to note that the high-energy sides of the spectra also match reasonably closely, giving credence to idea that the FE spectrum of TMA actually maps out the $\tilde{A} \leftarrow \tilde{X}$ transition. Not surprisingly, a calculation of the absorption spectrum based on displaced (0.50905 Å) harmonic oscillators ($\tilde{\nu}'' = 365$ cm^{-1}; $\tilde{\nu}' = 375$ cm^{-1}) also provided a reasonable fit to the observed spectrum. This follows from the presumption that the local minima of the ground-state potential energy surface are, within the range of thermally accesible, FC-mediated levels, reasonably harmonic. Moreover, the intrinsically large line width required by the TMA spectrum masks the relatively subtle anharmonicity of the bending potential.

Fluorescence Spectrum. The interesting and significant result of these calculations is that the fluorescence spectrum calculated

(16) B and x' depend on A, x_0, and K'' in the following way: for $n = 2$, $x' = \{K''(x_0)^2 - A\}/K''x_0$ and $B = k''(x_0/x' - 1)$; for $n = 4$, $2x' = 3x_0 - \{9(x_0)^2 - A/K''\}^{1/2}$ and $2B = k''\{x_0/(x')^3 - 1/(x')^2\}$.

(17) Geller-Leopold, D.; Halpern, A. M.; Vaida, V., unpublished data.

(18) Cureton, C. G.; Hara, K.; O'Connor, D. V.; Phillips, D. *Chem. Phys.* **1981**, *63*, 31.

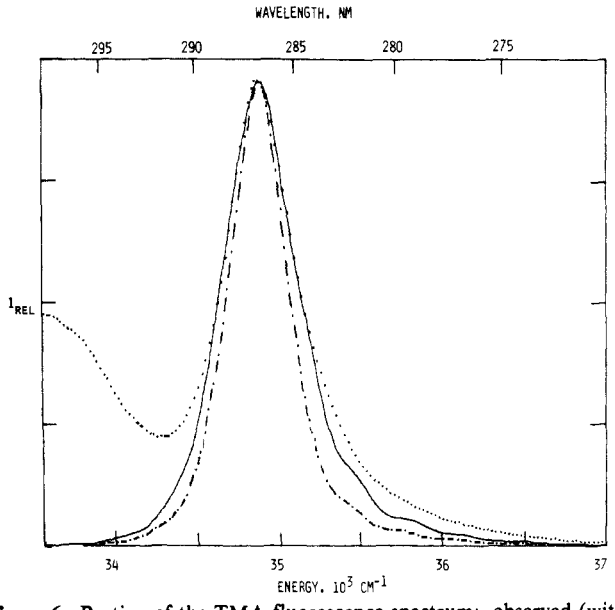

Figure 6. Portion of the TMA fluorescence spectrum: observed (with vibrational relaxation) (···); calculated spectrum with quadratic-capped potential (—); calculated with quartic-capped potential (-·-).

from the $\tilde{X}$ and $\tilde{A}$ state wavefunctions fits both the position and the narrow shape observed in TMA. This comparison can also be seen in Figure 5. In order to obtain a satisfactory alignment of the observed and calculated fluorescence spectra, the barrier height of the ground-state potential had to be chosen rather precisely (± ca. 20 cm^{-1}). The line width used in fitting the fluorescence spectrum was chosen to just barely damp out the "fine structure" until the observed line width of the (vibrationally relaxed) fluorescence was matched. This line width (ca. 300 cm^{-1}) was found to be smaller than that required to fit the absorption spectrum (ca. 460 cm^{-1}).

It thus appears that with respect to emission between the $\tilde{A}$ and $\tilde{X}$ states, FC intensity builds up rapidly over a rather narrow range of $\tilde{X}$ state levels (e.g., $v'' = 14$–18) and is responsible both for the narrowness and large Stokes' shift of the TMA fluorescence "origin" at 287 nm. This is documented in Table II, which contains the FC factors $\langle 0|v''\rangle^2$. It should be noted that the symmetry of the $\tilde{X}$ and $\tilde{A}$ state potentials requires that these FC factors vanish for odd v''. The FC values listed in Table 2 for odd v'' are indeed numerically very small and this attests to the reasonable quality of the calculation.

The calculations, as acknowledged above, obviously fail to take into account the remainder of the vibrational structure observed in the TMA fluorescence to the red of the "origin" at 287 nm. These other features appear to involve another ground-state vibrational mode (or modes) other than ν_7, such as N–C stretching in combination with the bending. A similarity exists, interestingly, in the absorption and emission (Raman) spectra of ammonia.[1c] A more complete treatment of the TMA emission spectrum obviously requires a two-dimensional analysis and will not be pursued further here. The rationale in omitting this interesting complication is that a one-dimensional approach is sufficient in explaining (1) the shape of the absorption spectrum, and (2) the large Stokes' shift and profile of the fluorescence "origin".

As mentioned above, the position of the (principal) fluorescence band depends strongly on the inversion barrier height. Accordingly, a barrier height of 2900 cm^{-1} is assigned for TMA. The width of the fluorescence band (given an intrinsic line width of 300 cm^{-1}, vide supra) was examined with the quadratic and parabolic caps in eq 1. These results are shown in Figure 6, which contains the observed principal fluorescence feature as well as the fluorescence spectra calculated with the quartic- and quadratic-capped potentials. In both cases the barrier height was chosen to allow the calculated spectra to coincide with the observed one. Thus barrier heights of 2925 and 2875 were used with the quadratic- and quartic-capped potentials, respectively. It can be seen in Figure 6 that, in order to achieve a comparably good fit using the quartic-capped potential, a larger line width is required. Since we cannot assign the intrinsic fluorescence line width with certainty, we are unable to determine which potential better models the inversion in TMA. A barrier height of ca. 2900 cm^{-1} is thus estimated for TMA.

It should be pointed out that the observed spectrum in Figure 6, while corrected for the detector response, is not multiplied by $\tilde{\nu}$, which is required for a rigorous comparison of our theoretical fluorescence spectra with the observed one.[19] Because of the narrow energy range covered by these spectra, this correction is of minimal consequence.

The inversion barrier height for TMA which we assign as 2900 cm^{-1} can be compared with values reported in the literature. Weston,[20] using a valence force field calculation, estimated the barrier height to be ca. 2860 cm^{-1}. Using the same force field approach, Koeppel et al.[21] obtained a value of 2610 cm^{-1}. More recently, Eades et al.[22] reported a barrier height of 3360 cm^{-1} for TMA based on a calculation using a large basis set, double-ζ with polarization. Thus the value that we assign falls between these estimates, which have been obtained from rather different approaches.

The calculations reported by Eades et al.[22] provide additional insight into the spectroscopy of TMA. They have suggested that methyl rotations are strongly coupled to inversion motion. Thus for electronic excitation that connects the pyramidal ground and planar excited states, methyl rotations represent an important degree of freedom. This was mentioned above in connection with the large line width used in the calculated absorption spectrum of TMA. This situation can be rationalized by the fact that in the pyramidal ground state, methyl rotations are strongly hindered (barrier height ca. 1500 cm^{-1}), whereas in the planar excited state there is apparently nearly free rotation of the methyl groups. Thus with respect to methyl rotations, electronic excitation involves a bound to continuum transition. The ground-state rotational barrier has been estimated by Fateley and Miller[23] from far-IR studies, while the near absence of this barrier stems from PRDDO-level calculations for planar TMA reported by Eades et al.[22] Thus cooling does not improve resolution due to large expected FC progressions in the hindered rotational (torsional) modes. This source of broadening does not exclude contributions from rapid intramolecular dephasing.

Assignment of the $\tilde{A}$–$\tilde{X}$ Origin. The electronic origin of the $\tilde{A} \leftarrow \tilde{X}$ transition was assigned by comparing the observed and calculated absorption spectra. These spectra were superimposed until the best fit, primarily on the low-energy side, was achieved. The origin obtained in this way is indicated in Figure 5 and corresponds to 37 550 cm^{-1}. Examination of the SD data in Table I shows that, indeed, there is a feature very close to this position (37 540 cm^{-1}) and it is identified by an arrow in Figure 4. This observation strengthens both the assignment of $\tilde{\nu}_{0\text{-}0}$ and the validity of the SD features.

Further support for this assignment is provided by the temperature dependence of the TMA absorption spectrum. As mentioned above, a feature in the SD spectrum can be identified at 287 nm, i.e., the fluorescence wavelength. While the intrinsic absorption strength at this energy, E_{abs}, is very low (i.e., 0.08 M^{-1} cm^{-1} at 300 K) due to the small population transitions to the $\tilde{A}$ state are readily enhanced because of the large FC factors associated with the $v'' = 14$–18 states (vide supra).

These absorption data are shown in Figure 7. The temperature dependence of the absorbance at this wavelength was studied between ambient temperature and 380 K. An Arrhenius plot of

(19) Birks, J. B. *Photophysics of Aromatic Molecules*, Wiley-Interscience: London, 1970; pp 84–87.
(20) Weston, R. E., Jr. *J. Am. Chem. Soc.* **1954**, *76*, 2645.
(21) Koeppel, G. W.; Sagatys, D. S.; Krishnamurthy, G. S.; Miller, S. I. *J. Am. Chem. Soc.* **1967**, *89*, 3396.
(22) Eades, R. A.; Well, D. A.; Dixon, D. A. *J. Phys. Chem.* **1981**, *85*, 976.
(23) (a) Rinehart, E. A.; Rinehart, P. B.; Wollrab, J. E. *J. Mol. Spectrosc.* **1973**, *47*, 556.
(24) (b) Fateley, W. G.; Miller, F. A. *Spectrochim. Acta* **1962**, *18*, 977.

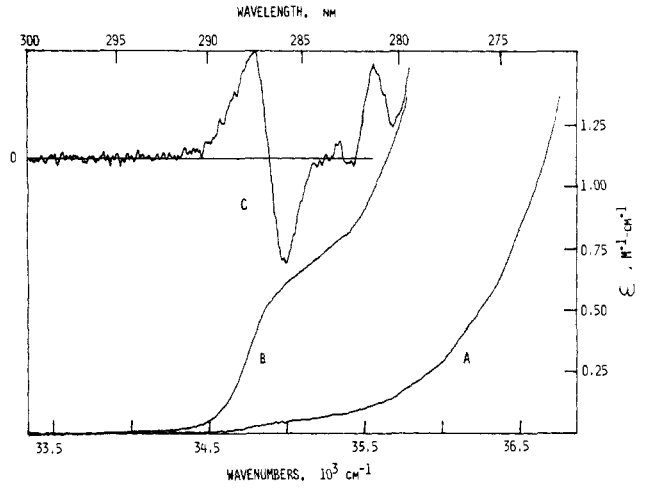

Figure 7. (A) Absorption spectrum of TMA vapor at 300 K (600 torr, 10-cm pathlength); (B) at 380 K; (C) second-derivative spectrum of B.

these data is linear and provides an activation energy (E_{act}) of 2700 cm^{-1}. From this value, $\tilde{\nu}_{0-0}$ can be estimated as $E_{abs} + E_{act}$, i.e., 37 501 cm^{-1}. This value is in good agreement with that obtained from the fitting of the $\tilde{A} \leftrightarrow \tilde{X}$ spectra (i.e., 37 550 cm^{-1}). Also, the barrier height, determined from $A = E_{act} + {}^1/_2\tilde{\nu}_7$, i.e., 2883 cm^{-1}, agrees well with that obtained from fitting the spectra (2900 cm^{-1}).

Conclusion

The shapes of the absorption and fluorescence spectra of TMA can be calculated with reasonable accuracy with a simple model along the out-of-plane bending mode. This model is based on one-dimensional potentials for the ground and lowest excited states, for which the normal coordinate is taken to be the TMA pyramid height. A ground-state potential that is successful in reproducing the position and shape of the fluorescence spectrum is a pair of local harmonic wells smoothly joined by a quadratic or quartic cap. As suggested by the absorption spectrum, the upper state can be represented by a harmonic potential. Calculations confirm that the large Stokes' shift and narrow line shape associated with TMA fluorescence can be attributed to transitions that terminate in a narrow range of highly excited ground-state inversion levels that are near the top of the barrier. Accordingly, both the height and (in some cases) the shape of the barrier to inversion can be probed by the fluorescence spectrum. We find that for TMA, a parabolic- or quartic-capped barrier height of ca. 2900 cm^{-1} can account for the position and shape of the fluorescence spectrum relative to absorption. The investigation of other barrier heights for other flexible amines using emission analysis techniques appears to be a promising approach. For example, the fluorescence spectrum of triethylamine suggests that the inversion barrier in this amine is considerably lower than that for TMA. The application of this technique to rigid amines such as 1-azabicyclo-[2.2.2]octane (ABCO), per se, is inappropriate because this amine does not have a ground-state double-minimum potential.

Experimental Section

TMA, obtained from Matheson Gas, was trap-to-trap distilled and then freeze–pump–thaw degassed before use. Absorption and derivative spectra were obtained on a Varian 2300 spectrophotometer (bandpass 0.3 nm). Fluorescence spectra were measured with a dc fluorimeter equipped with a 150-W Xe lamp. The relaxed fluorescence spectrum (4 torr TMA) was obtained through the use of ca. 100 torr of 2-methylbutane as the buffer gas. Excitation was at 230 nm; bandpass, 2-nm excitation and 0.5-nm emission. The TMA fluorescence excitation spectrum (2 torr) was corrected with a sodium salicylate screen and was monitored at 287 nm; the excitation bandpass was 0.4 nm.

Both spectrometers were interfaced to a DEC LSI 11/03 microcomputer for further data analysis. The finite-difference program and spectrum-generating routines were run on a VAX 11/780 computer.

Acknowledgment. This work was partially supported by the donors of the Petroleum Research Fund, administered by the American Chemical Society (A.M.H. and M.J.O.) and by the National Science Foundation (L.D.Z.). A helpful conversation with Professor E. B. Wilson is gratefully acknowledged. E. Reid provided valuable assistance with computer programming.

Appendix

If x is the domain of a function, F, such that $\mathbf{x} = (x_1, x_2, ..., x_N)$, where $x_{i+1} = x_i + \Delta x$, and $\mathbf{F} = \{F(x_1), F(x_2), ..., F(x_N)\}$, then

$$\mathbf{F}'' = (1/\Delta x)^2 \begin{pmatrix} -2 & 1 & & & 0 \\ 1 & -2 & 1 & & \\ & 1 & -2 & 1 & \\ & & 1 & -2 & 1 \\ 0 & & & 1 & -2 \end{pmatrix} \mathbf{F}$$

The Schrödinger equation

$$-F'' + (2m/\hbar^2)VF = (2m/\hbar^2)EF$$

where V is the potential energy function that spans x is solved numerically from the diagonalization of the tridiagonal matrix having diagonal elements

$$H_{ii} = 2/\Delta x^2 + (2m/\hbar^2)V_i$$

and subdiagonal elements

$$H_{i,i-1} = -1/\Delta x^2$$

The eigenvectors are the eigenfunctions F_i, and the eigenvalues are equal to $(2m/\hbar^2)E_i$.

Registry No. TMA, 75-50-3.